Dynamics of capillary condensation in aerogels

R. Nomura, W. Miyashita, K. Yoneyama, and Y. Okuda
Department of Condensed Matter Physics, Tokyo Institute of Technology, 2-12-1 O-okayama, Meguro, Tokyo 152-8551, Japan
(Received 13 July 2005; revised manuscript received 24 January 2006; published 8 March 2006)

Dynamics of capillary condensation of liquid ^{4}He in various density silica aerogels was investigated systematically. Interfaces were clearly visible when bulk liquid was rapidly sucked into the aerogel. Time evolution of the interface positions was consistent with the Washburn model and their effective pore radii were obtained. Condensation was a single step in a dense aerogel and two steps in a low density aerogel. Crossover between the two types of condensation was observed in an intermediate density aerogel. Variety of the dynamics may be the manifestation of the fractal nature of aerogels which had a wide range of distribution of pore radii.

DOI: 10.1103/PhysRevE.73.032601 PACS number(s): 67.40.Hf, 47.56.+r, 67.20.+k, 68.03.−g

Liquid-gas phase transition in porous material is suitable for studying the basic problem of the effects of disorder on phase transitions and critical phenomena, and has been suggested to be a realization of the random field Ising model [1,2]. Liquefaction processes of ^{4}He in silica aerogels have been studied extensively [3–9]. Aerogels are very tenuous materials with fractal correlation in nanometer scales [10–12] and have various porosities. They provide an opportunity to study the effect of correlated disorder on liquid-gas phase transitions in a systematic and controllable way. Hysteresis was observed in adsorption and desorption of ^{4}He, and was recently reproduced by simulation in realistic aerogel structures [13,14]. To date experiments have been performed slowly to study the adsorption process in quasiequilibrium or in rate-independent limit [3–8].

In this paper we condensed ^{4}He very rapidly, avoiding liquefaction in aerogels, in order to study how aerogels with different porosities sucked up the outside liquid. Interfaces were observed during the condensation into aerogels under this highly nonequilibrium condition. The motion of the interfaces was described by the Washburn model [16] and effective pore radii were obtained. Condensation in a dense aerogel was a single-step process with a single interface, while condensation in a low density aerogel was two-step process with two interfaces appearing separately. Crossover between the two processes was observed in the temperature dependence for an intermediate density aerogel. These behaviors may be the manifestation of the fractal character of aerogels with no well-defined pore radii. The two-step capillary condensation is probably related to the avalanche process of liquid in aerogels referring to the studies under quasiequilibrium conditions.

The experiment was performed in a ^{3}He optical cryostat as described in Ref. [9]. A sample cell with two windows was anchored to the ^{3}He pot and we could observe its inside from room temperature. Temperature was measured by a RuO_2 resistance thermometer inside the cell. We used silica aerogels of three porosities, ϕ=90.4, 95.8, and 99.5% which were made by MarkeTech International Inc., USA [15]. In this paper these samples are referred to as aerogels P90, P96, and P99. Their heights were about 12 mm. One of the aerogels was set on a stage fixed on the bottom of the cell. The rate of filling ^{4}He gas in the cell f was controlled by a needle valve of a gas handling system at room temperature. One might worry about the large temperature gradient in aerogels caused by the large heat release from the adsorbed few monolayers of ^{4}He. The monolayers always existed before the rapid filling began because they were not completely evacuated between each filling. We expect that they did not cause the temperature gradient during filling. We investigated the dynamics of capillary condensation in aerogels at a high filling rate in the temperature range of 2.2 to 4.2 K where liquid ^{4}He was normal fluid.

At a low filling rate of ^{4}He gas, the aerogel became almost uniformly opaque during the condensation before the bulk liquid appeared outside of the aerogel. As condensation proceeded, it cleared up and became transparent again, and was filled with the liquid completely. Then, bulk liquid appeared outside of the aerogel. This behavior at low filling rate was common to all the aerogels of different porosities used in our experiment. An extensive optical study was reported by Lambert *et al.* [5] who observed behavior similar to ours.

At a high enough filling rate, however, equilibrium was not established in the aerogel and bulk liquid appeared outside of the aerogel before it became opaque. A bulk liquid-gas interface outside of the aerogel rose as the condensation proceeded in the cell. Once the interface reached the bottom of the aerogel, the aerogel sucked the liquid. The liquid-gas interface in aerogel was visible and rose much faster than the bulk interface did. Successive images of this process are shown in Fig. 1 for P90. The filling rate was f =4.8 μmol/sec and temperature was T=2.4 K; this was about 70 times faster than the case in which the aerogel

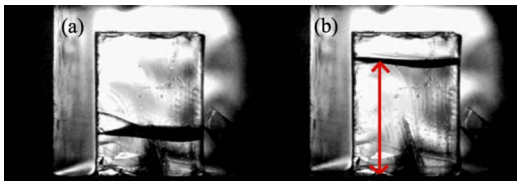

FIG. 1. (Color online) Single-step capillary condensation of liquid ^{4}He in aerogel P90 at 2.4 K. The arrow indicates the height of the interface. Times of the images are (a) 0.37 and (b) 3.47 min.

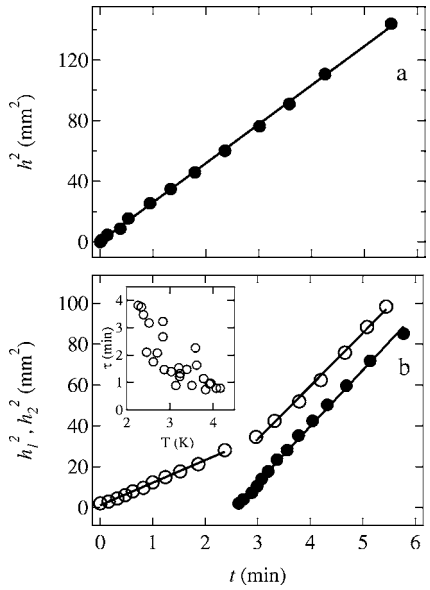

FIG. 2. (a) Time evolution of the height of the interface for aerogel P90 at 2.4 K. (b) Time evolution of h_1 and h_2 (see text) for aerogel P96 at 2.5 K. Lines in the figures are the fitting by Eq. (1). Inset is the temperature dependence of the catch-up time τ.

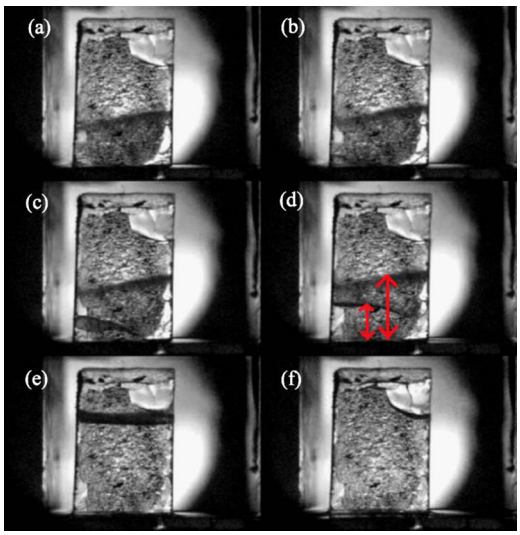

FIG. 3. (Color online) Two-step capillary condensation of liquid ^{4}He in aerogel P96 at 2.5 K. The right (left) arrow indicates the height h_1 (h_2) of the precursor (second) interface. Times of each image are (a) 1.87; (b) 2.23; (c) 2.60; (d) 2.97; (e) 4.68; (f) 6.42 min.

became opaque. Height of the interface h was measured at a particular position as indicated by the arrow in Fig. 1 and h^2 is plotted as a function of time t in Fig. 2(a). We can clearly see $h^2 \propto t$. This single-step capillary condensation was observed throughout the experimental temperature range for P90. We always found $h^2 \propto t$ and the interface moved faster at lower temperatures.

Different dynamics was observed at large f for the lower density aerogels P96 and P99. We followed the same procedure described above to fill the cell without making the aerogel opaque and the aerogel sucked the liquid in two steps as can be seen in Fig. 3. In this case, the aerogel was P96 and $T=2.5$ K. Again, a bulk liquid-gas interface outside of the aerogel rose as the condensation proceeded, and the aerogel began to suck up the liquid when the interface reached the bottom of the aerogel. Initially a precursor interface with a height of h_1 rose in the aerogel. The second interface with a height h_2 appeared later, rose in the aerogel faster than the precursor interface and caught up with it; thereafter the precursor interface moved at the same speed as the second interface. We define τ as the time at which the second interface caught up with the precursor interface and call the process before (after) $t=\tau$ step 1 (2). In Fig. 2(b), time evolution of h_1 and h_2 are plotted as open and closed circles and $\tau \approx 3.2$ min in this case. We can see that ${h_1}^2 \propto t$ both in step 1 and 2 and that ${h_2}^2 \propto t$.

The behavior $h^2 \propto t$ is consistent with the Washburn model of capillary condensation in porous media [16,17]. The model assumes that the liquid with viscosity η flows in a narrow capillary with radius R following Poiseuille's law and that the driving force for the flow is the capillary pressure $\Delta P = 2\gamma \cos\theta / R$. Here, γ is surface tension and θ is the contact angle of the liquid. The Washburn equation is

$$h(t)^2 = \frac{\gamma R \cos\theta}{2\eta} t. \tag{1}$$

We extracted the effective radius of the pore size at each temperature using Eq. (1) from the known values of $\eta(T)$ [18] and $\gamma(T)$ [19] for ^{4}He. We assumed complete wetting by liquid ^{4}He: $\theta=0$. Figure 4 is a plot of the effective radii of

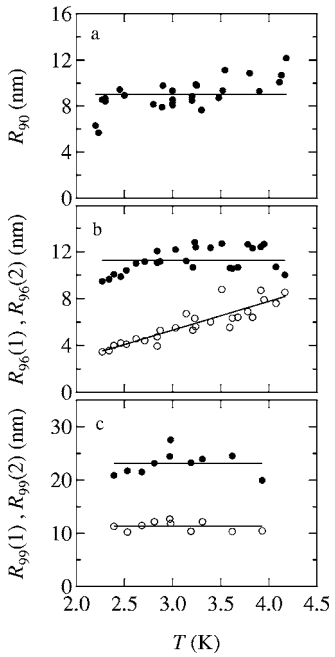

FIG. 4. Temperature dependence of the effective radii of aerogels P90 (a), P96 (b), and P99 (c). Closed circles are obtained from h or h_2 and open circles are from h_1 (see text). Lines are the guides for the eyes.

three aerogels at different temperatures. Condensation in P90 was a single step and the single value of the effective radius R_{90} was obtained from $h(t)$. In P96 condensation was two steps and thus we had two effective radii: $R_{96}(1)$ obtained from $h_1(t)$ in step 1 and $R_{96}(2)$ from $h_2(t)$. In the same way we had $R_{99}(1)$ and $R_{99}(2)$ for P99.

In an ordinary porous material with a well-defined pore size, the Washburn model gives a single value of the pore radius which does not depend on the properties (η and/or γ) of working liquids. Propriety of the Washburn model for aerogels is not clear because aerogels do not have a particular pore radius. Although interface motions were about 2.5 times faster at the lowest temperature 2.2 K than at 4.2 K mostly due to the temperature dependence of $\gamma(T)$, R_{90} was scaled to be an almost temperature independent value, $R_{90}=9.0\pm1.4$ nm, as in Fig. 4(a) using $\eta(T)$ and $\gamma(T)$. This implies, surprisingly, that the Washburn model seemed to derive correctly the relevant scale of pores in the low porosity aerogel where condensation of liquid was a single step. R_{90} may be around the largest scale of pore size because the aerogel was completely filled with the single-step.

As for the two-step condensation observed in lower density aerogels, step 1 was presumably the process at which a precursor liquid, whose front was at h_1, first flowed in the regions with a higher density of silica strands, where the effective pore radius was smaller and the liquid could exist more stably. Step 2 was the process at which the liquid filled the space with the largest pore size where it was harder for the liquid to exist. Two values of the effective pore radii for the single aerogel does not mean that the aerogels had two well-defined subnetworks but rather that the fractal nature of the aerogels which have large distributions in pore radii led to the two-step condensation. It is reasonable that $R_{96}(2)$ had a temperature independent value 11.3 ± 1.1 nm and was larger than R_{90} as can be seen in Fig. 4(b). However, $R_{96}(1)$ had a very curious temperature dependence. This is because $h_1(t)$ was almost temperature independent in P96. $R_{96}(1)$ was less than half of $R_{96}(2)$ at 2.3 K and was close to $R_{96}(2)$ at 4.2 K. This means that the precursor liquid flowed through pores of different scales depending on the temperature. The temperature dependence may be the manifestation of the fractal character of the aerogel structure, otherwise the effective pore size would have been a specific value. In the inset of Fig. 2(b), τ is plotted as a function of temperature. The period of step 1 became shorter at higher temperatures as τ decreased with increasing temperature. Therefore, the condensation in P96 was two steps $[R_{96}(1)<R_{96}(2)]$ at low temperatures and became single step like those $[R_{96}(2)\approx R_{96}(1), \tau\approx 0]$ at high temperatures. As for the lowest density aerogel P99, the condensation was always two steps and we had two temperature independent effective radii, $R_{99}(1)=11.3\pm1.0$ nm and $R_{99}(2)=23.1\pm2.1$ nm.

Types of the capillary condensation in aerogels are summarized as follows: single step for the dense aerogel P90, two-steps for the low density aerogel P99, and single step like at high temperatures and two steps at low temperatures for the intermediate porosity aerogel P96. What controls the dynamics of capillary condensation? Fluid dynamics in a confined geometry with fractal correlation is a very complicated problem and not much is known about it. Let us refer to the studies on adsorption of ^{4}He in aerogels under quasi-equilibrium conditions which have been extensively investigated experimentally [4–8] and theoretically [13,14] in order to gain insight into our highly nonequilibrium situation. Shapes of adsorption isotherms of ^{4}He in aerogels change with porosities and temperatures as follows. Densities of ^{4}He in aerogels increase by increasing chemical potential μ to the bulk equilibrium value or by increasing pressure to the bulk equilibrium vapor pressure. This increase is gradual at higher temperatures or in denser aerogels and has a sharp jump at a particular chemical potential μ_c at lower temperatures or in lower density aerogels. The jump becomes larger and μ_c becomes smaller at lower temperatures or for higher porosities. This behavior was recently reproduced by the lattice model of a fluid within local mean-field theory [13,14]. Aerogel structure was generated by a diffusion-limited cluster-cluster aggregation algorithm which is believed to reproduce the structural features of aerogels [10–12]. It was shown that increasing temperature mimicked decreasing porosity for the shapes of adsorption isotherms. The gradual change in density observed at higher temperatures or in low porosities was a process in which the liquid layer coating the aerogel strands thickens continuously and finally fills the pore smoothly as μ increased. The jump in the isotherm observed at lower temperatures or in higher porosities was associated with macroscopic avalanches of liquids at $\mu=\mu_c$. Liquids are formed in the dense strand regions or in the pores with small size below μ_c and almost completely fill the large pore regions abruptly with macroscopic avalanches at $\mu=\mu_c$. The avalanches were the origin of the hysteresis in adsorption and desorption. Complex behaviors of the isotherms can be recognized as a manifestation of the fractal nature of aerogels, not seen in the other dense porous materials. So far clear experimental observation of the avalanche process has been reported only in the draining of superfluid ^{4}He in Nuclepore [20].

In a situation in which the avalanche process is involved, dynamics of the capillary condensation may become two steps. Liquid needs a finite driving force associated with μ_c to flow in the largest pore region. However, before the large pores are filled, precursor liquid can flow in the small pore region without any threshold value for the driving force. One can notice that the conditions of porosity and temperature for the two-step capillary condensation are similar to those for the jump in the isotherms or the macroscopic avalanches. If we regard step 1 as the process of precursor liquid flowing in the dense strand regions and step 2 as the liquid filling the large pore regions with macroscopic avalanches, the observed dynamics can be qualitatively explained. For the dense aerogel P90 condensation was single step because liquid could fill the pores smoothly without any abrupt change. For the low density aerogel P99 it had two-step condensation at all temperatures because it always had to have avalanches. For the intermediate case of P96 it was two-step condensation at low temperatures where the avalanche process had to be involved and was single step like at high temperatures where the liquid could fill the pores more smoothly. Temperature dependences of $R_{96}(1)$ and τ were caused by the crossover between the two condensation mechanisms. There-

fore, our finding of the several types of capillary condensation may be another way of manifestation of the fractal nature of aerogel. It is, of course, necessary to check this scenario not just by the similarity to the results in quasiequilibrium but by a theory dealing with the dynamical process positively.

We investigated the dynamics of capillary condensation in aerogels with various porosities at high filling rates. Aerogels sucked the outside liquid from the bottom by making interfaces. Condensations were a single step for the dense aerogel, two steps with two separated interfaces for the low density aerogel, and single step like at high temperatures and two steps at low temperatures for the intermediate porosity aerogel. The height of the interface proceeded as $\sqrt{t}$ in both single step and two steps, and the effective pore radii were obtained from the Washburn model. Two-step condensation was possibly the consequence of avalanches referring to the experiments and the theories under quasiequilibrium condition. Variety of the dynamics may be a manifestation of the fractal nature of aerogels which had a wide range of distribution of the pore radii. The determination of the spatial distribution of the average ^{4}He density in aerogels, the investigation of the sample dependence and the sample characterization are remaining as the future subjects. These measurements are necessary to make our interpretation more solid.

We are grateful to Y. Lee for helping us to prepare aerogels. This study was partly supported by a 21st Century COE Program at TokyoTech "Nanometer-Scale Quantum Physics" and by the Grants-in-Aid for Scientific Research from the Ministry of Education, Culture, Sports, Science, and Technology of Japan.

[1] F. Brochard and P. G. de Gennes, J. Phys. (Paris), Lett. **44**, 785 (1983).
[2] P. G. de Gennes, J. Phys. Chem. **88**, 6469 (1984).
[3] A. P. Y. Wong and M. H. W. Chan, Phys. Rev. Lett. **65**, 2567 (1990).
[4] C. Gabay, F. Despetis, P. E. Wolf, and L. Puech, J. Low Temp. Phys. **121**, 585 (2000).
[5] T. Lambert, C. Gabay, L. Puech, and P. E. Wolf, J. Low Temp. Phys. **134**, 293 (2004).
[6] J. R. Beamish and T. Herman, Physica B **329**, 340 (2003).
[7] J. R. Beamish and T. Herman, J. Low Temp. Phys. **134**, 339 (2004).
[8] T. Herman, T. Day, and J. Beamish, Phys. Rev. B **72**, 184202 (2005).
[9] W. Miyashita, K. Yoneyama, R. Nomura, and Y. Okuda, J. Phys. Chem. Solids **66**, 1509 (2005).
[10] A. Hasmy, E. Anglaret, M. Foret, J. Pelous, and R. Jullien, Phys. Rev. B **50**, 6006 (1994).
[11] J. V. Porto and J. M. Parpia, Phys. Rev. B **59**, 14583 (1999).
[12] T. M. Haard, G. Gervais, R. Nomura, and W. P. Halperin, Physica B **284**, 289 (2000).
[13] F. Detcheverry, E. Kierlik, M. L. Rosinberg, and G. Tarjus, Phys. Rev. E **68**, 061504 (2003).
[14] F. Detcheverry, E. Kierlik, M. L. Rosinberg, and G. Tarjus, Langmuir **20**, 8006 (2004).
[15] 4750 Magnolia Street, Port Townsend, WA 98368, USA.
[16] E. W. Washburn, Phys. Rev. **17**, 273 (1921).
[17] T. M. Squires and S. R. Quake, Rev. Mod. Phys. **77**, 977 (2005).
[18] K. N. Zinoveva, Sov. Phys. JETP **34**, 421 (1958).
[19] K. R. Atkins, *Liquid Helium* (Cambridge University Press, Cambridge, 1959).
[20] A. H. Wootters and R. B. Hallock, Phys. Rev. Lett. **91**, 165301 (2003).